



MASTER OF SCIENCE PROGRAM
IN PHYSICS OF COMPLEX SYSTEMS

Chaos and ergodicity in quantum systems

Author:

Carlotta Nunzi

Supervisor:

Fabrizio Dolcini
Politecnico di Torino,

Co-Supervisor:

Andrea de Luca
Université de Cergy-Pontoise

*Ad Ame e a Sam
A Vicio e a Sharon
A Persia e a Noe
E a tutti quelli che.*

Contents

1	The model	3
1.1	Localisation for $q = 2$ - 1D case	6
1.2	Localization for $q = 3$ - Cayley tree	10
2	A stochastic recurrence relation	13
2.1	Moments	13
3	A numerical approach	15
3.1	Population dynamics	15
3.2	Sampling the s values	16
3.3	Numerical distributions	16
3.4	Moments	18
4	Conclusions	21
A	Directed polymer on a tree	23
B	Importance sampling	27

Introduction

The Anderson localisation, in its simplest form, is the absence of diffusion of waves in a disordered medium. It was first introduced in 1958 [1] by Philip W. Anderson and it is at the very basis of many condensed matter phenomena.

Prior to quantum mechanics, the study of conductance of electrons followed Drude theory for which free electrons are scattered by positive ions in metal lattice sites [2]. The mean free path is intended as the average length an electron travels before it is scattered by an ion and this quantity was assumed to be directly proportional to electronic conductivity.

With quantum mechanics, physicists were able to understand that electrons do not scatter from ions that occupy lattice sites. The scattering is due to the wave nature of electrons and to the presence of imperfections in the crystal.

What Anderson discovered is that increasing the presence of impurities not only electrons scatter more frequently, diminishing the length of their free path and so the conductivity, but there is a certain impurity limit after which electrons become trapped in their positions and the system in question becomes insulating.

In this work we explore a mean-field version of the Anderson localisation phenomena, where we substitute the usual regular lattice $2d$ or $3d$ lattice with a Cayley-tree graph [3], the finite size limit of a Bethe Lattice system. The model, introduced in [3], studies the behavior of waves propagating on a tree and it assumes two simplifications. Firstly, waves can propagate only in one direction, breaking time reversibility (like electrons moving in an external magnetic field). Secondly, the phase shifts arising from scattering are assumed to be identical and independent random variables, to model the impurities in a real system.

A single parameter θ controls the strength of the scattering of the waves and consequently the nature of eigenstates. The study is based on testing the sensitivity of energy levels with respect to local spatial perturbations. This said sensitivity can be seen to be related to the amplitude of the corresponding eigenstate in the perturbed region. A useful result is a non-linear integral recursion for the probability distribution of eigenstate amplitudes for an increasing size system.

1 The model

The model is that of waves propagating and scattering along the structure of a Cayley tree.

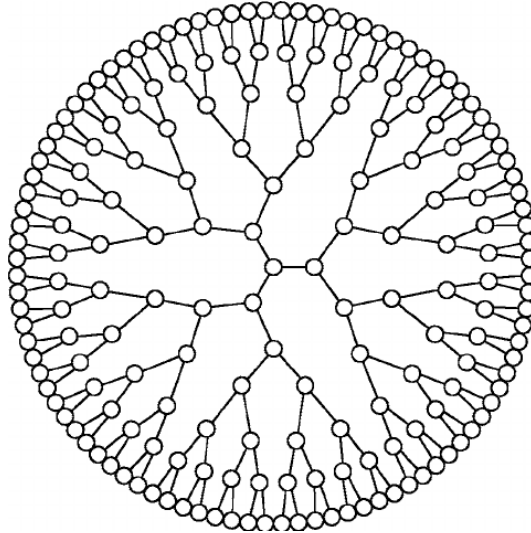


Figure 1: Cayley tree graph.[4]

The model is built by links and nodes, no specific Hamiltonian is given: the study is carried out knowing that along each link the scattered wave gains a phase shift and at the node four waves meet and the scattering happens and is represented by a scattering matrix.

For these reasons the quantities of interest are $z(s)$ which is defined as the amplitude along a link and $|z(s)|^2$ which is the corresponding flux.

Taken a random link n that starts in s_1 and ends in s_2 , the phase gain for every $z(s_1)$ is:

$$z(s_2) = \exp(i\psi_n)z(s_1) \quad (1)$$

where ψ_n is the phase shift associated to the link n .

Taken a random node n where four links meet: two of them carry incoming fluxes and two of them carry outgoing fluxes. For $z(s_1)$, $z(s_2)$, $z(s_3)$ and $z(s_4)$ the scattering matrix will be:

$$\begin{pmatrix} z(s_1) \\ z(s_3) \end{pmatrix} = \mathbf{M} \begin{pmatrix} z(s_4) \\ z(s_2) \end{pmatrix} \quad (2)$$

where the matrix \mathbf{M} specifies the scattering happening at the node. The shape of the Matrix is forced by the conservation of the flux:

$$|z(s_1)|^2 - |z(s_3)|^2 = |z(s_4)|^2 - |z(s_2)|^2 \quad (3)$$

which leads to:

$$\mathbf{M} = \begin{pmatrix} e^{i\alpha} & \\ & e^{i\beta} \end{pmatrix} \begin{pmatrix} \cosh\theta & \sinh\theta \\ \sinh\theta & \cosh\theta \end{pmatrix} \begin{pmatrix} e^{i\gamma} & \\ & e^{i\delta} \end{pmatrix} \quad (4)$$

with $\alpha, \beta, \gamma, \delta$ and θ taken real. By choice of a certain rotation of the system the only parameter that defines the scattering is $\theta \geq 0$.

$$\mathbf{M}(\theta) = \begin{pmatrix} \cosh\theta & \sinh\theta \\ \sinh\theta & \cosh\theta \end{pmatrix} \quad (5)$$

The angle varies between $\theta = 0$ and $\theta = \infty$ taking the model through its mobility edge. The two limit values of θ correspond respectively to the situation in which states are extended and the same flux flows over every link and the situation in which states are localised and the network splits into a large number of separated loops. These two extreme situations are described in the following figures:

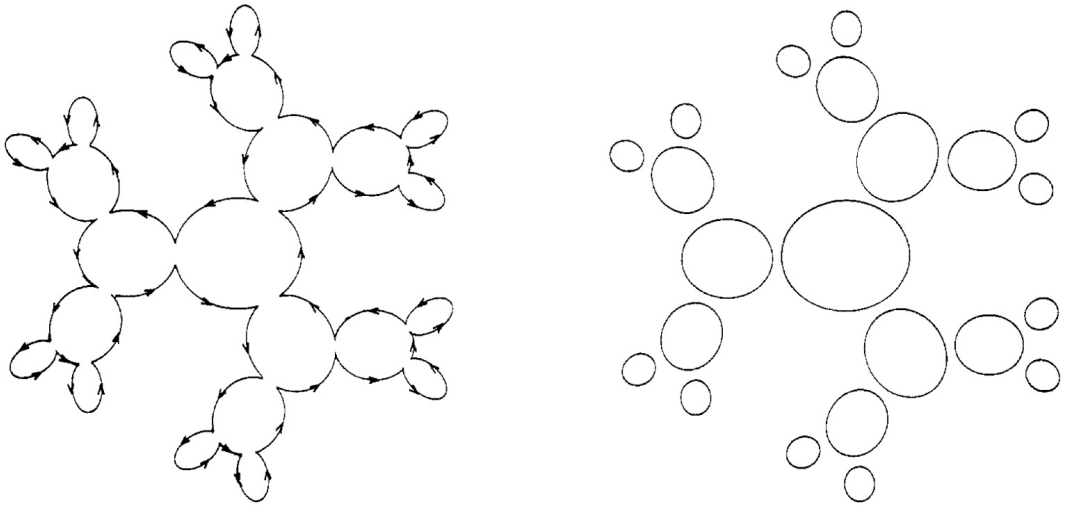


Figure 2: The two graphs represent extreme values assumed by θ . On the left, $\theta = 0$ and the flux flows over every link in the direction indicated by the arrows. On the right, $\theta = \infty$ and the tree has split into a big number of separated loops. [3]

Most of the study is done analytically, for this reason are picked networks that allow this. A first explanation of the model is done for $q = 2$ (where q stands for the coordination

number of the nodes of the graph) and then is presented a generalisation for $q = 3$ that can be extended also to cases with higher q -value.

The link phases have a direct correlation with the allowed eigenvalues of the system and for this reason they cannot be chosen in an arbitrary way, they must be able to satisfy both 1 and 4. To find the relation between phase shifts and energy, is made the ansatz that the link phases vary much more rapidly than the scattering parameter that, in a narrow energy range, can be considered fixed. The assumption is of linear variation of the phase shift with energy:

$$\psi_n = \alpha_n + \beta_n E \quad (6)$$

where the only source of randomness is in α_n whereas β_n is taken constant. The random variable α_n can assume every value in the range $[0, 2\pi)$.

The solution to this model leads both to the eigenvalues and eigenvectors and to the allowed amplitudes $z(s)$ along the graph. The main goal of the study is to find these solutions as a function of the scattering parameter θ .

The procedure to find the eigenvalues of the system is to build a set of amplitudes $z(s)$ that obeys the equation 1 and 4 everywhere apart from one link. The result will be a term $\Psi(E)$ carrying out all the phases through the graph and a term α_N representing the random shift along the last link. To get an eigenvalue the following condition must be satisfied:

$$\Psi(E_l) + \alpha_N = 2\pi l \quad (7)$$

where l is an integer.

The nature of the corresponding eigenstates is found by studying the sensitivity of the energy levels with respect of small changes of the random phase α_N [5]. From 7 this sensitivity is related to the gradient of $\Psi(E)$:

$$-\left(\frac{dE_l}{d\alpha_N}\right)^{-1} = \left[\frac{\partial\Psi(E)}{\partial E}\right] \Big|_{E=E_l} \quad (8)$$

The behaviour of the probability distributions can be explained by looking at the phase $\Psi(E)$ as a function of the energy:

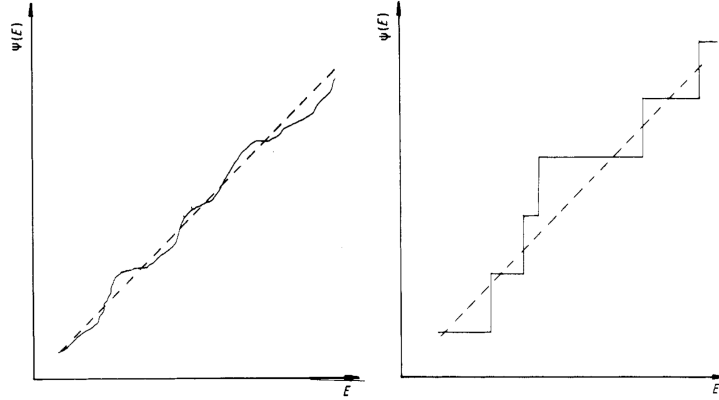


Figure 3: [3] Behaviour of the phase function $\Psi(E)$ as a function of the energy: in the right plot when states are extended, in the left plot when states are localised.

In the extended case, as the energy varies, the phase doesn't change much. This translates in a *p.d.f.* with a gaussian shape (Figures 7) where it is possible to move between a small range of gradient values.

In the localised case, a small energy perturbation can lead to a big phase difference. The corresponding *p.d.f.* will then have a power law behaviour as observed in Figure 9.

1.1 Localisation for $q = 2$ - 1D case

What has been discussed so far is now applied to a 1 dimensional network:

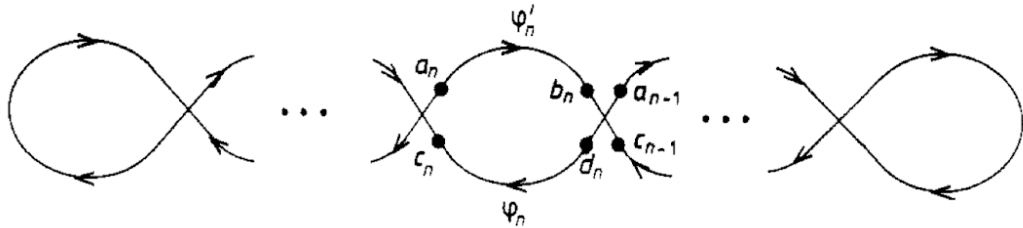


Figure 4: Diffusion model on a 1D Cayley tree.[3]

The approach used consist in trying to build an eigenstate of energy E along the network of figure 4 by matching the values of successive $z(s)$ going right to left. This matching work is done neglecting the last link where the eigenstate nature will be determined by the condition 7.

Equations 1 and 4 for amplitudes at successive points now become:

$$z(a_n) = \exp(-i\psi'_n)z(b_n) \quad z(c_n) = \exp(i\psi_n)z(d_n) \quad (9)$$

and

$$\begin{pmatrix} z(b_n) \\ z(d_n) \end{pmatrix} = \mathbf{M}(\theta) \begin{pmatrix} z(a_{n-1}) \\ z(c_{n-1}) \end{pmatrix}. \quad (10)$$

The relation between phases and energy is now:

$$\psi_n + \psi'_n = \alpha_n + E \quad (11)$$

where α_n are still iid random variables that can assume values in the range $[0, 2\pi)$ and E is the energy. Looking back at the relation 7, it is needed to keep track of the phase difference along the network, which is equal to:

$$\psi_n = \arg[z(c_n)] - \arg[z(a_n)]. \quad (12)$$

This phase difference can be expressed as a function of ψ_{n-1} and α_n .

As a consequence of flux conservation it is possible to define:

$$\arg[z(d_n)] - \arg[z(b_n)] = 2\tan^{-1}[e^{-2\theta}\tan(\psi_{n-1}/2)] \equiv g(\theta, \psi_{n-1}) \quad (13)$$

and from the relation between phases and subsequent links 9:

$$\psi_n = \alpha_n + E + g(\theta, \psi_{n-1}). \quad (14)$$

Additionally, from the scattering matrix equation 10 one can get, as a function of $g(\theta, \psi)$:

$$\left| \frac{z(a_{n-1})}{z(a_n)} \right|^2 = \frac{\partial g(\theta, \psi_{n-1})}{\partial \psi_{n-1}}. \quad (15)$$

At this point the eigenvalues are determined by the condition 7 that in an N loop chain becomes:

$$\psi_N(E_l) = 2\pi l \quad (16)$$

which in this model leads to:

$$\Psi(E) = \psi_N(E_l) - \alpha_N. \quad (17)$$

To understand the type of eigenvalue, the approach that this study follows is that to study the typical gradient of 16. From the total derivative of 17 one finds that the partial gradient of 16 wrt to the energy leads to a recursion relation obtained differentiating 14:

$$\frac{\partial\psi_n}{\partial E} = 1 + \frac{\partial g(\theta, \psi_{n-1})}{\partial\psi_{n-1}} \frac{\partial\psi_{n-1}}{\partial E} \quad (18)$$

with the initial condition $\partial\psi_1/\partial E = 1$.

At fixed energy, successive ψ_n are uncorrelated, because of this the values $\partial g(\theta, \psi_{n-1})/\partial\psi_{n-1}$ are independently distributed at every step of the recursion relation. Iterating 18 and using 15 it is found that:

$$\frac{\partial\psi_N}{\partial E} = \frac{\left(\sum_{n=1}^N |z(a_n)|^2\right)}{|z(a_n)|^2} \quad (19)$$

and, by choosing $\sum_{n=1}^N |z(a_n)|^2 = 1$ for a normalised eigenstate, one gets the following powerful relation:

$$-\frac{dE_l}{d\alpha_N} = |z(a_N)|^2. \quad (20)$$

The relation means that the sensitivity of an energy level to a perturbation of a given link phase is proportional to the total flux flowing on that link.

To carry out further analysis of the model two averages are introduced. Up until now it has been studied $\psi_N(E)$ as a function of energy for a specific realisation of the disorder α_N . It is easier to consider instead the probability distribution of $\partial\psi_N(E)/\partial E$ when the energy is fixed over the entire ensemble of realisation of the disorder. The probability that there is an eigenstate at the level of the chosen energy, given that α_N is distributed uniformly, is proportional to $\partial\psi_N(E)/\partial E$.

The two mentioned averages in the ensemble are the following. The average of a generic quantity X at fixed E over all realisations of the disorder independently of whether the system has an eigenstate at said E is defined as $\langle X \rangle_0$. The average restricted to the systems in the ensemble that have eigenstates at the energy E considered is indicated by $\langle X \rangle$. The two averages are related in the following way:

$$\langle X \rangle = \frac{\langle X(\partial\psi_N(E)/\partial E) \rangle_0}{\langle \partial\psi_N/\partial E \rangle_0}. \quad (21)$$

Using these two averages and the recursion relation 18 it can be shown that states are localised in a one dimensional network.

To do this one looks at the moments of the recursion relation starting from the definition of $g(\theta, \psi)$ 13.

$$\left\langle \frac{\partial g(\theta, \psi)}{\partial \psi} \right\rangle_0 = \frac{1}{2\pi} \int_0^{2\pi} [e^{2\theta} \cos^2(\psi/2) + e^{-2\theta} \sin^2(\psi/2)]^{-1} d\psi = 1 \quad (22)$$

and

$$\left\langle \left(\frac{\partial g(\theta, \psi)}{\partial \psi} \right) \right\rangle_0 = \frac{1}{2\pi} \int_0^{2\pi} [e^{2\theta} \cos^2(\psi/2) + e^{-2\theta} \sin^2(\psi/2)]^{-2} d\psi = \cosh(2\theta) \quad (23)$$

Knowing this one can average over the recursion relation and get the first two moments of 18:

$$\langle \partial\psi_N/\partial E \rangle_0 = N \quad \langle (\partial\psi_N/\partial E)^2 \rangle_0 \propto \cosh(2\theta)^N. \quad (24)$$

The fact that the second moment of 18 grows exponentially in N while the first moment grows only linearly in N indicates that states are localised. This can also be deduced by the fact that $\langle |z(a_n)|^{-2} \rangle$ grows exponentially whereas for uniformly extended states $\langle |z(a_n)|^{-2} \rangle = N$.

A more complete way to arrive to the same result would be to consider directly the probability distribution of the phase gradient $\rho(x)$ (where $x = \partial\psi_N/\partial E$). Since the magnitude studied is $x \geq 1$ either a limiting distribution exists for large N or the typical values of x diverge with N .

Assuming that a limiting distribution exists would imply, because $\langle x \rangle_0$ diverges with N , that $\rho(x)$ cannot fall more rapidly than x^{-2} as $x \rightarrow \infty$.

To prove the existence of $\rho(x)$, it has to be demonstrated that there are bounded moments of x as $N \rightarrow \infty$. To do so the following inequality is exploited:

$$(1+x)^y \leq 1+x^y \quad (25)$$

true when $x \geq 0$ and $0 \leq y \leq 1$. Using the notation: $\partial\psi_N/\partial E = x_n$ and $\partial g(\theta, \psi)/\partial \psi = s$, the inequality is applied to the recursion relation (18) getting:

$$\begin{aligned} \langle (x_n)^y \rangle_0 &= \langle (1 + sx_{n-1})^y \rangle \leq 1 + \langle (sx_{n-1})^y \rangle = 1 + \langle s^y \rangle \langle (x_{n-1})^y \rangle \\ \langle (x_n)^y \rangle_0 &\leq \sum_{k=0}^{n-1} \langle s^y \rangle^k = \frac{1 - \langle s^y \rangle^N}{1 - \langle s^y \rangle} \end{aligned} \quad (26)$$

Knowing that $0 < \langle s^y \rangle < 1$ when $0 < y < 1$ implies that $\langle (x)^y \rangle$ remains bounded as $N \rightarrow \infty$. This result means that a limiting distributions with all integers moments infinite exists. The *p.d.f.* will be given by:

$$\rho(x) = \int ds \int dx' P(s) \rho(x') \delta(sx' + 1 - x) \quad (27)$$

where $P(s)$ is the *p.d.f.* of s .

1.2 Localization for $q = 3$ - Cayley tree

The introduction of the mathematical approach done for the 1D system allows now to study the network model defined on a Cayley tree with three n.n. to each loop as shows Figure1.

The goal is to get the *p.d.f.* of the eigenstates amplitudes. In this configuration, four regimes are identified as the scattering parameter θ is varied.

The model is defined as the 1D case but with the changes that come from having three n.n. instead of two.

The phase differences are given by:

$$\begin{aligned}\psi_{n-1} &= \arg[z(a_1)] - \arg[z(a_2)] & \psi'_{n-1} &= \arg[z(b_1)] - \arg[z(b_2)] \\ \psi_n &= \arg[z(c_1)] - \arg[z(c_2)]\end{aligned}\quad (28)$$

and recursion relation on the phase difference now becomes:

$$\psi_n = \alpha_n + E + g(\theta, \psi_{n-1}) + g(\theta, \psi'_{n-1}) \quad (29)$$

where α_n is a phase associated to the loop n .

The relation on successive amplitudes is now:

$$|z(a_1)/z(c_1)|^2 = \partial g(\theta, \psi_{n-1}) / \partial \psi_{n-1}. \quad (30)$$

The relation on the very last phase difference at the centre of the tree is given by:

$$\Psi = E + g(\theta, \psi_{N-1}) + g(\theta, \psi'_{N-1}) + g(\theta, \psi''_{N-1}) \quad (31)$$

and, in order to identify an eigenvalue, that has to satisfy:

$$\Psi(E) + \alpha_N = 2\pi l. \quad (32)$$

The study is, once again, carried out studying the sensitivity of energy levels to a local perturbation (8).

The recursive relation on a Cayley tree is:

$$\frac{\partial \psi_n}{\partial E} = 1 + \frac{\partial g(\theta, \psi_{n-1})}{\partial \psi_{n-1}} \frac{\partial \psi_{n-1}}{\partial E} + \frac{\partial g(\theta, \psi'_{n-1})}{\partial \psi'_{n-1}} \frac{\partial \psi'_{n-1}}{\partial E} \quad (33)$$

with I.C. $\partial \psi_1 / \partial E = 1$.

The first moment of the phase gradient is:

$$\langle \partial \Psi / \partial E \rangle_0 = 3 \times 2^{N-1} - 2. \quad (34)$$

Acquired this result, instead of studying the moments of the phase gradient, one finds directly the *p.d.f.* $\rho_n(x)$ of $x = \partial \psi_n / \partial E$ as a whole. When $N \rightarrow \infty$ either x is bounded and so it exists a limiting distribution or typical values increase with N .

When x increases with n , given the result in (34), one expects that $x \sim O(a^n)$ with $a \leq 2$.

In the following, will be illustrated the four localisation regimes depending on the values assumed by the scattering parameter.

REGIME 1: $\theta \in [\theta_1, \infty]$. Using the same inequality as in (25) and proceeding in the same way, it can be demonstrated that $\langle (\partial \psi_n / \partial E)^y \rangle_0$ is bounded as $N \rightarrow \infty$ when $y \in [0, 1]$ and provided that $2f(y) < 1$ where $f(y) \equiv \langle [\partial g(\theta, \psi) / \partial \psi]^y \rangle_0$. This inequality is satisfied for $y = 1/2$ if $\theta > \theta_1$ with $\theta_1 = 1.88$.

In this case exists a limiting distribution $\rho(x)$ and it satisfies an equation analogous to (27):

$$\rho(x) = \int \int \int \int dx_1 dx_2 ds_1 ds_2 P(s_1) P(s_2) \rho(x_1) \rho(x_2) \delta(x - 1 - s_1 x_1 - s_2 x_2) \quad (35)$$

where $P(s)$ is the probability distribution of $\partial g(\theta, \psi) / \partial \psi$.

Inserting the trial form for $n \rightarrow \infty$ $\rho(x) \sim Ax^{-\alpha}$, α is determined by $f(\alpha - 1) = 1/2$.

Large values of θ correspond to strong disorder, meaning that the first regime represents a localised case. It can be supposed that all states have the square modulus that decays exponentially $Be^{-n/\xi}$ where n is the distance from the centre. These states are normalizable provided that $2e^{-1/\xi} < 1$. The normalization condition comes from the following geometric series:

$$\sum_{n=0}^{N-1} 2^n e^{-n/\xi} = \sum_{n=0}^{N-1} (2e^{-1/\xi})^n \quad (36)$$

where the first term in the sum is the number of states at distance n from the origin of the Cayley tree. Assuming for the centres of the states to be uniformly distributed, the fluxes have form $y = Be^{-n/\xi}$ where $n = 0, 1, \dots, N - 1$ with probabilities $P_n = 2^{n-N}$. It is possible to go from this probability to the probability $\mu(y)$ by doing a change of variables $P_n dn = \mu(y) dy$. With the change of variables $\mu(y) \propto 2^{-N} 1/y^\beta$ where $\beta = 1 + \xi \ln 2$ and $Be^{-(N-1)/\xi} < y < B$. In the strong scattering limit where $\theta = \infty$ the correlation length is equal to zero and $\alpha = 2$.

REGIME 2: When $\theta_2 < \theta < \theta_1$ with $\theta_2 \simeq 0.881$ the condition for the limiting distribution is no longer valid and so typical values increase exponentially with n .

Instead of studying directly $\partial\psi_n/\partial E$, one studies t_n where $t_n = \frac{1}{b^n}\partial\psi_n/\partial E$:

$$t_n = 1 + \frac{1}{b} \left(\frac{\partial g(\theta, \psi_{n-1})}{\partial \psi_{n-1}} t_{n-1} + \frac{\partial g(\theta, \psi'_{n-1})}{\partial \psi'_{n-1}} t'_{n-1} \right) \quad (37)$$

with $t_1 = 1$. Comparing the recursive relation for t_n and the recursive relation for $\partial\psi_n/\partial E$, $t_n > b^{-n}\partial\psi_n/\partial E$.

Having already seen that $\partial\psi_n/\partial E \sim O(a^n)$, t_n will have a limiting distribution when $n \rightarrow \infty$ as long as $b > a$. With a study analogous to that of the REGIME 1, inserting the trial asymptotic form $At^{-\alpha}$ into the recursive relation for t_n , the condition on α is given by $f(\alpha - 1) = \frac{1}{2}b^{\alpha-1}$.

REGIME 3: $\theta_3 < \theta < \theta_2$ with $\theta_3 \simeq 0.347$ corresponds to eigenstates whose square modulus goes like the inverse of the system size, indicating that states are no longer localized, but whose distribution of values is a power tail. This coincides with the case where $\partial\psi_n/\partial E \sim 2^n$ ($a = 2$) so, in order to have a limiting distribution for the large n case, it has to be defined $r \equiv 2^{-n}(\partial\psi_n/\partial E)$:

$$r_n = \frac{1}{2} \left(\frac{\partial g(\theta, \psi_{n-1})}{\partial \psi_{n-1}} r_{n-1} + \frac{\partial g(\theta, \psi'_{n-1})}{\partial \psi'_{n-1}} r'_{n-1} \right). \quad (38)$$

In this regime r has a limiting distribution $\pi(r)$, substituting the trial form of $\pi(r) \sim Ar^{-\alpha}$ into the definition of $\pi(r)$ leads to the condition on α which is then determined by $f(\alpha - 1) = 2^{\alpha-2}$.

REGIME 4: $0 < \theta < \theta_3$, also in this case $\partial\psi_n/\partial E \sim 2^n$. The difference with the previous regime is that now $\pi(r)$ falls more rapidly to zero with increasing r than any negative power of r , this assures that all positive integers moments of r are finite.

2 A stochastic recurrence relation

A more in dept and generalized study can be done for the equation 33. In the most general case possible, the recursion relation (33) can be rewritten as:

$$x_n = 1 + \sum_{p=1}^K s_{n-1}^{(p)} x_{n-1}^{(p)} \quad (39)$$

where $x = \partial\psi(E)/\partial E$ and $s = \partial g(\theta, \psi)/\partial\psi$.

Solving (33) it is possible to get the moments of x_n .

2.1 Moments

The variable s are obtained, as mentioned in 22, from an angle $\phi \in [0, 2\pi]$ uniformly distributed:

$$s(\phi) = \frac{1}{e^{2\theta} \cos^2(\phi) + e^{-2\theta} \sin^2(\phi)} \quad (40)$$

Is thus possible to identify its first moment $\rho(1) = 1$ and its second moment is $\rho(2) = \cosh 2\theta$.

The k -th moment of of the variable s will be denoted as $\rho(k)$. Using $\rho(k)$ it is possible to compute exactly the moments of x_n defined as $\rho_n(k)$.

For the average, denoted by $\rho_n(1)$:

$$\rho_{n+1}(1) = 1 + 2\rho(1)\rho_n(1) \quad (41)$$

which yields:

$$\rho_n(1) = (2\rho(1))^{n+1} - 1 \quad (42)$$

assuming $x_0 = 1$. Since $\rho(1) = 1$, it reduces to:

$$\rho_n(1) = 2^{n+1} - 1 \quad (43)$$

This shows that the average is never bounded.

For the second moment, already, it can be observed a richer behaviour:

$$\rho_{n+1}(2) = 1 + 2\rho(2)\rho_n(2) + 4\rho(1)\rho_n(1) + 2\rho(1)^2\rho_n(1)^2 \quad (44)$$

$$\rho_{n+1}(2) = 2\rho(2)\rho_n(2) + (1 + 2\rho(1)\rho_n(1))^2 \quad (45)$$

There are two distinct contributions to the recursion of $\rho_n(2)$ one which contributes as $(2\rho(2))^n$ and the second growing as 4^n . For large n , thus, it is expected:

$$\rho_n(2) \sim 2^{n\tau_2} \quad (46)$$

with

$$\tau_2 = \max\left\{2, \frac{\ln 2\rho(2)}{\ln 2}\right\} \quad (47)$$

Hence, in this case, is expected a change in τ_2 for $\cosh 2\theta > 2$, $\theta > \frac{1}{2} \ln(2 + \sqrt{3}) \approx 0.66$. For higher moments, one expects a similar behaviour where now it is assumed $\rho_n(q) \sim 2^{n\tau_q}$ with:

$$\tau_q = \max\left\{q, \frac{\ln 2\rho(q)}{\ln 2}\right\} \quad (48)$$

These results will be now tested with a numerical approach based on population dynamics, a Monte Carlo method to simulate random variables with a recurrence structure.

In appendix we discuss, moreover, an alternative way to tackle this recurrence equations, showing its link with the problem of directed polymers in random media.

3 A numerical approach

3.1 Population dynamics

The stochastic recurrence relation 39, in the specific case of $K = 2$, can be numerically tackled (at least for small n) by adopting a population dynamics sampling method. The algorithm is based on the idea that, to sample a value at step $n + 1$, we just need to know two independent values at step n .

The population dynamics works as follows:

- At step $n = 0$ is initialized a list of values $x_0 = [1, \dots, 1]$ of size N_{pop} .
- At any time step n it is considered the current list $x_n = [x_n^{(1)}, \dots, x_n^{(N_{\text{pop}})}]$. It is created a new list of the same size x_{n+1} as follows:

$$x_{n+1}^{(i)} = 1 + s_1 x_n^{(i_1)} + s_2 x_n^{(i_2)} \tag{49}$$

where the indices i_1 and i_2 two random indices drawn independently from the set $1 \dots N_{\text{pop}}$ and s_1, s_2 are drawn each time from:

$$s = [e^{2\theta} \cos^2 \phi + e^{-2\theta} \sin^2 \phi]^{-1} \tag{50}$$

where ϕ is uniformly distributed in $[0, 2\pi]$.

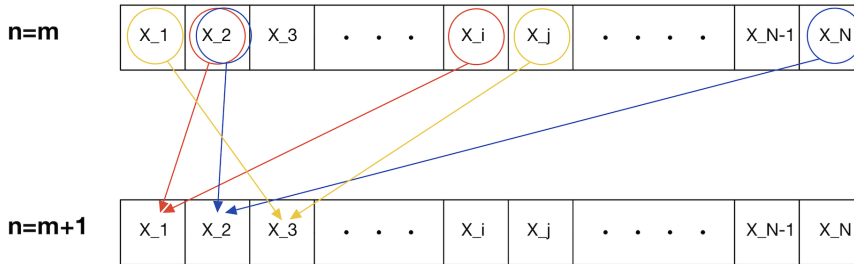


Figure 5: First step of the creation of the new population.

The idea is the following: values at each time step are not strictly independent but, by taking a large enough N_{pop} , the growing correlations can be contained. As these correlations grow with n , effectively N_{pop} limits the maximum n reachable. This problem can be mitigated by running multiple independent population dynamics runs and averaging among those.

3.2 Sampling the s values

As previously anticipated, at each step two independent values of s_i are drawn from 50. Below is reported the C++ code snippet used:

```
double new_s(double angle, std::default_random_engine& generator1){
    std::uniform_real_distribution<double> distribution(0.0,2*M_PI);
    double phi=0;
    double new_s=0;

    phi=distribution(generator1);

    return new_s=1/(exp(2*angle)*pow(cos(phi),2)+ exp(-2*angle)*pow(sin(phi),2));
}
```

Figure 6: C++ code used to extrapolate values of s

3.3 Numerical distributions

Thanks to the numerical use of population dynamics, it was possible to extrapolate the probability distribution of x_n at different time steps n and for different values of θ belonging to the four different regimes previously identified. In the following the four distributions will be shown:

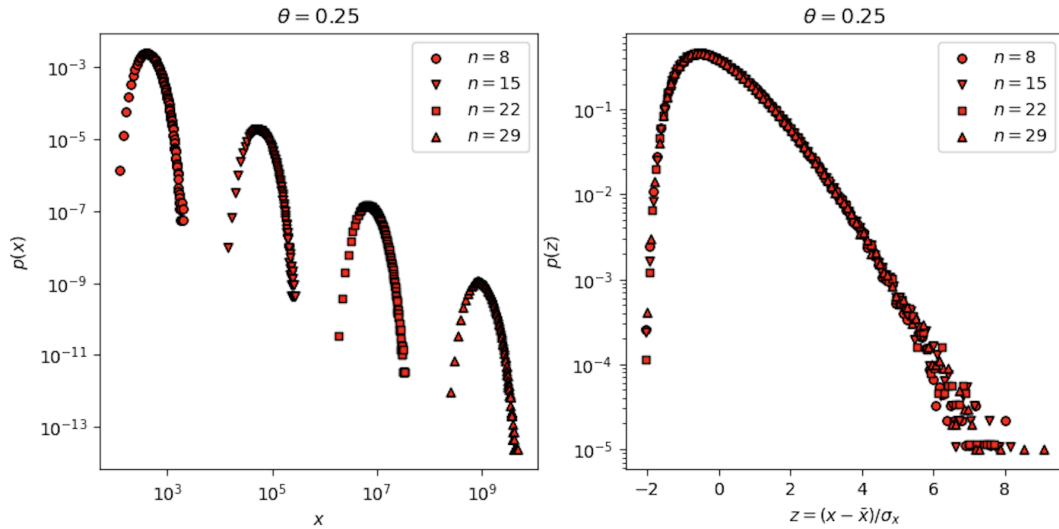


Figure 7: The two plots show the p.d.f. of x when $\theta = 0.25$. Only a limited number of n are shown to appreciate the general behaviour. On the left the different distributions are shown in a *log-log* scale to highlight how they move at different n . On the right, the *log* scale is removed from the *x-axis* and a collapse of the distributions can be seen.

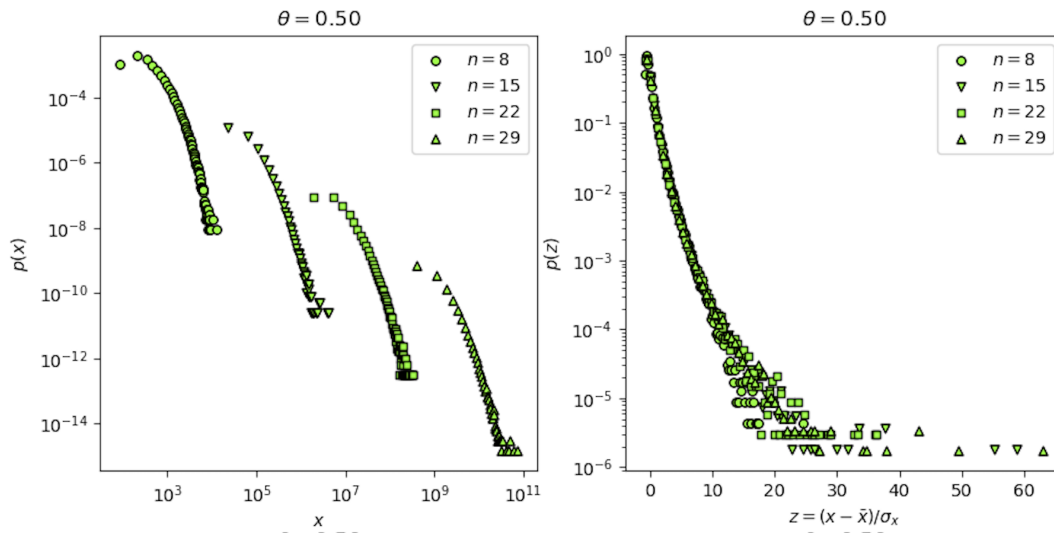


Figure 8: The two plots show the p.d.f. of x when $\theta = 0.50$. Only a limited number of n are shown to appreciate the general behaviour. On the left the different distributions are shown in a *log-log* scale to highlight how they move at different n . On the right, the *log* scale is removed from the x -axis and a collapse of the distributions can be seen.

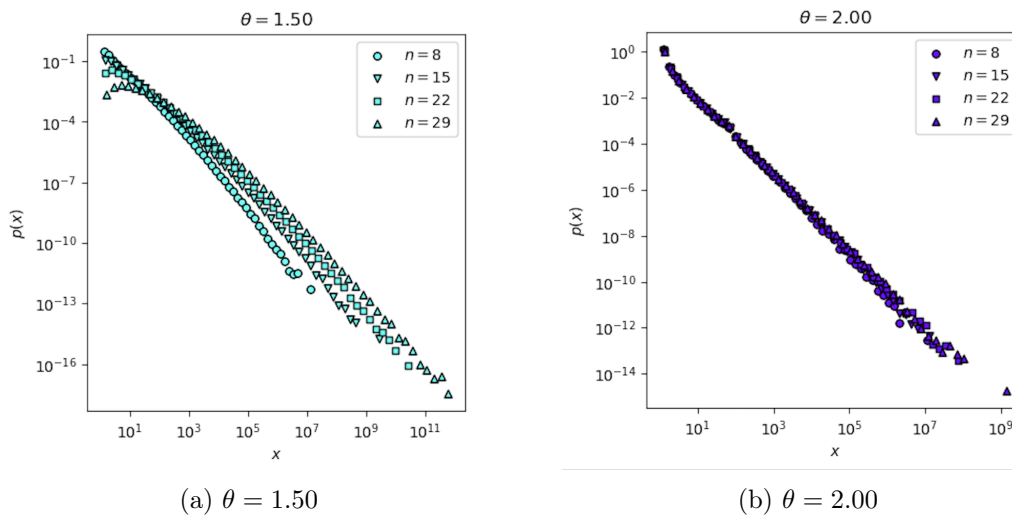


Figure 9: Both p.d.f.s are presented in *log-log* scale plots. On the left is the case of $\theta = 1.50$ whereas on the right there's the distribution for $\theta = 2.00$.

In the images is highlighted the evolution of the distribution along all the time steps where $n \in [0, 30]$.

Something happens when removing the mean from all datasets and dividing by the standard deviation, it is possible to observe that when $\theta = 0.25$ and $\theta = 0.5$ there is a collapse in the distribution at different time steps. The collapse means that the

distributions corresponding to these two regimes are well concentrated around the mean value.

For $\theta = 1.5$ and $\theta = 2$ it is experienced a different behaviour, it can be observe a collapse of the distributions at different time-steps that becomes more clear and defined for $\theta = 2$. This collapse implies that in this two regimes, especially for bigger values of θ , a limiting distribution is reached, in agreement with the theoretical results 35.

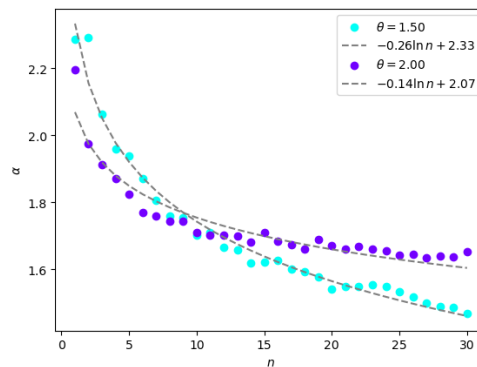


Figure 10: Fitted power law exponents from the distributions obtained in figure 9 with varying n . The obtained scaling is compatible with a logarithmic decay of the exponent as n grows, compatible with the slow convergence in the high theta regime. The origin and the study of such exponent is left as future work.

3.4 Moments

With the same population dynamics approach it is possible to extrapolate the numerical behaviour of the first and the second moment of the distributions for the different θ as a function of the time-steps n :

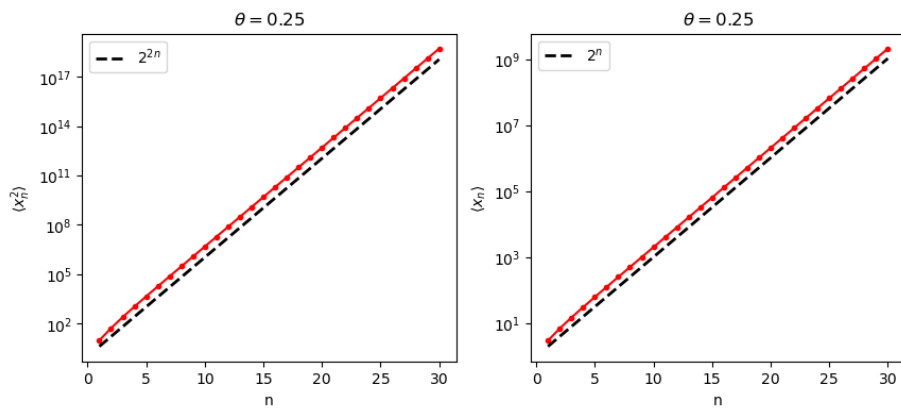


Figure 11: From left to right: second and first moment of the distribution for $n \in [0, 30]$ and $\theta = 0.25$.

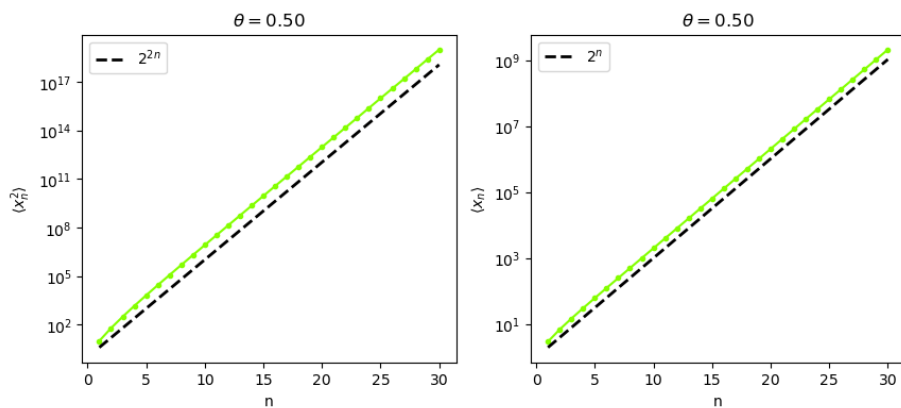


Figure 12: From left to right: second and first moment of the distribution for $n \in [0, 30]$ and $\theta = 0.50$.

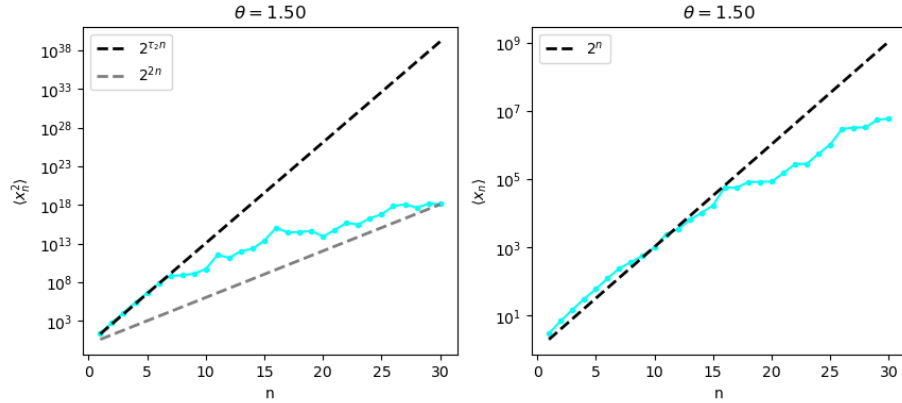


Figure 13: From left to right: second and first moment of the distribution for $n \in [0, 30]$ and $\theta = 1.50$.

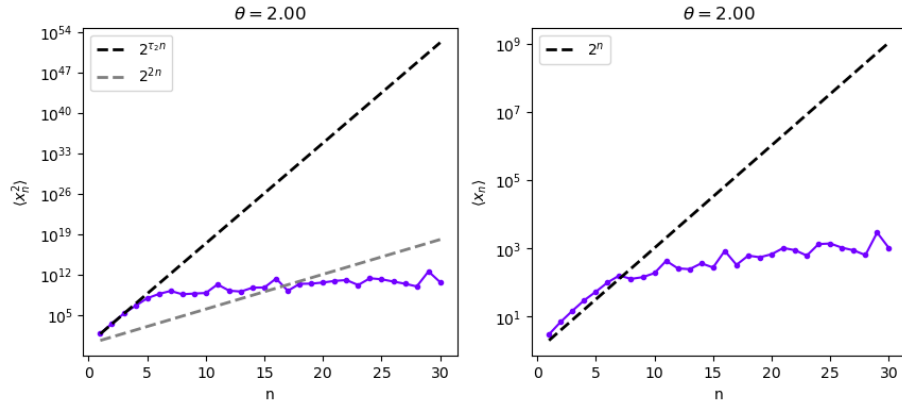


Figure 14: From left to right: second and first moment of the distribution for $n \in [0, 30]$ and $\theta = 2.00$.

From this study, it is possible to observe how for $\theta = 0.25$ and $\theta = 0.50$ the population dynamics works perfectly and the numerical data align with the theoretical expectation line. This behaviour could have been anticipated by the previous numerical analysis: these two regimes are well distributed around the mean so the numerical sampling works well.

A different behaviour is observed when $\theta = 1.5$ and $\theta = 2$, in this case population dynamics fails to reproduce the theoretical results. The reason for this result being that these two distributions are not well centered around the mean and more efficient numerical methods should be used.

4 Conclusions

This thesis discussed a model of Anderson localisation, which resulted in the study of the stochastic recurrence relation 39. First were presented results from the original literature that show how the recurrence relation 33 can be obtained from a scattering model of waves propagating along a Cayley Tree. From this model of propagation four different scattering regimes emerged corresponding to different values of the scattering parameter θ . The model is first presented in its simplest $1D$ -form and then in the $3D$ case where the actual regimes emerge.

The recurrence relation 39 is then analysed in a more systematic way in order to extrapolate the analytical values of the first moments of the distribution for x that will be later compared with the numerical simulations.

A numerical study is led to recover the analytical result presented in the previous sections. The method used is that of population dynamics. The use of this method limits the number of step for the evolution of the population to a low number that in this case corresponds to $n_{steps} = 30$. The probability distributions of x at different value of θ are recovered. For small values of θ , $\theta = 0.25$ and $\theta = 0.50$, it can be observed how the p.d.f. changes for different values of n , also, removing the average and dividing for the standard deviation, it can be noticed how the different p.d.f.s all collapse in a single one meaning that for different n the distributions are well concentrated around the mean. For bigger values of θ , $\theta = 1.50$ and especially $\theta = 2.00$, different behaviour is observed, at different values of n the p.d.f.s collapse indicating the presence of a limiting distribution, as predicted by the theory.

Following the the numerical approach, an evaluation of the first two moments of the distribution is given. For small values of θ ($\theta = 0.25$ and $\theta = 0.50$) the population dynamics method is sufficient to capture the behaviour as a function of n and the numerical evaluation agrees with the theoretical results. This is because, as previously demonstrated, the corresponding distributions are well-defined around the mean value. For bigger values of θ ($\theta = 1.50$ and $\theta = 2.00$) the population dynamics method fails to capture the correct behaviour of the first two moments for bigger values of n , in this case, a different numerical approach is required.

Moreover, in the appendix, a generalization of this stochastic problem was presented, alongside its link with the problem of directed polymer in random media originating from statistical physics.

Finally, an idea on how to solve the sampling problem for high θ regimes is discussed in the second appendix, introducing an Importance Sampling method.

References

- [1] Philip W Anderson. Absence of diffusion in certain random lattices. *Physical review*, 109(5):1492, 1958.
- [2] Ad Lagendijk, Bart van Tiggelen, and Diederik S Wiersma. Fifty years of anderson localization. *Physics today*, 62(8):24–29, 2009.
- [3] JT Chalker and S Siak. Anderson localisation on a cayley tree: a new model with a simple solution. *Journal of Physics: Condensed Matter*, 2(11):2671, 1990.
- [4] Ted Brookings, J Carlson, and John Doyle. Three mechanisms for power laws on the cayley tree. *Physical review. E, Statistical, nonlinear, and soft matter physics*, 72:056120, 12 2005.
- [5] David J Thouless. Electrons in disordered systems and the theory of localization. *Physics Reports*, 13(3):93–142, 1974.
- [6] Mehran Kardar, Giorgio Parisi, and Yi-Cheng Zhang. Dynamic scaling of growing interfaces. *Phys. Rev. Lett.*, 56:889–892, Mar 1986.
- [7] B. Derrida and H. Spohn. Polymers on disordered trees, spin glasses, and traveling waves. *Journal of Statistical Physics*, 51(5):817–840, Jun 1988.
- [8] M. Bramson. *Convergence of Solutions of the Kolmogorov Equation to Traveling Waves*. 1983.
- [9] B. Derrida. The random energy model. Technical report, France, 1980. CEA-CONF-5131.
- [10] Extreme value statistics and traveling fronts: various applications. *Physica A: Statistical Mechanics and its Applications*, 318(1):161–170, 2003. STATPHYS - Kolkata IV.
- [11] Satya N. Majumdar and P. L. Krapivsky. Extremal paths on a random cayley tree. *Phys. Rev. E*, 62:7735–7742, Dec 2000.
- [12] Satya N. Majumdar and P. L. Krapivsky. Extreme value statistics and traveling fronts: Application to computer science. *Phys. Rev. E*, 65:036127, Feb 2002.

A Directed polymer on a tree

The stochastic recursion relation presented in chapter 2 has strong similarities with one emerging from a well-known model in the statistical physics of disordered systems, namely the directed polymer (DP) in random media [9, 7]. In its original version, a DP is a directed path in a $d + 1$ dimensional lattice indexed by a "time" or "length" variable t and taking values in the lattice sites x . See figure 15 for an example depiction.

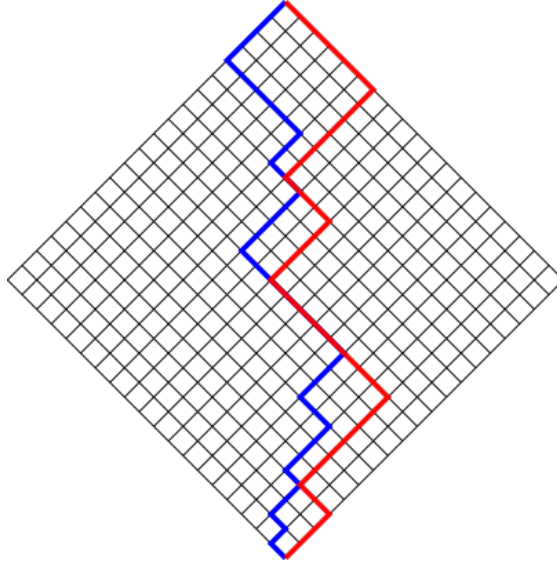


Figure 15: Directed polymer in 1 + 1 dimensions. Example of directed path, from top to bottom. Each step in towards the end of the lattice goes from $t \rightarrow t + 1$ and $x \rightarrow x \pm 1$.

The "random medium" parts refers to the fact that one associates to each lattice site (x, t) a quenched random variable $V_{x,t}$ which models the local disorder of the system. As such, each path of length n in the lattice has an associated energy:

$$E_n = \sum_{t \leq n} V_{x(t),t} \quad (51)$$

As the $V_{x,t}$ are random variables, E_n are also. It is possible to study the statistics of the path's energies by translating the problem to a statistical physics problem i.e. by introducing the partition function:

$$Z_{\text{DP}} = \sum_{\{x(t)\}} e^{-\beta \sum_{t \leq n} V_{x(t),t}} \quad (52)$$

where the sum is taken along all the possible paths and β is the inverse temperature. Exact results for the 1 + 1 dimensional DP are available and are linked to the KPZ universality class [6]. Much less is known for $d \geq 2$.

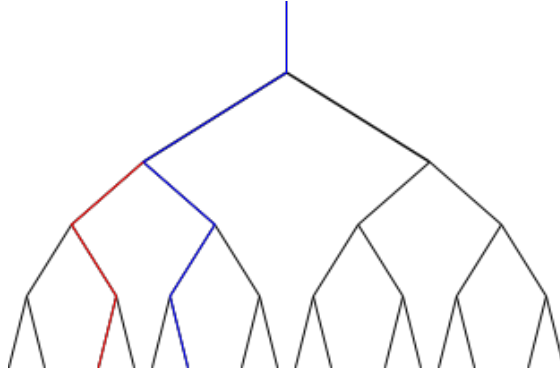


Figure 16: Directed polymer on a tree dimensions. Example of two directed paths, from top to bottom. Each step in towards the end of the lattice goes from $t \rightarrow t + 1$ and goes either left or right.

Due to the difficulties of the problem, Derrida and Spohn introduced in [7] a mean-field like version of the DP, by considering paths on a tree. The energy has the same form as the $d + 1$ DP however the problem of studying Z_{DP} is more amenable as:

- Paths in a tree do not intersect after separating
- The tree structure induces simple recurrence relation on the observables

Indeed, the energy of a path in a (binary) tree with $t + 1$ levels can be decomposed to

$$E_{t+1} = V + E_t^{(1)} + E_t^{(2)} \quad (53)$$

where $E_t^{(1)}$ and $E_t^{(2)}$ are energies of two paths each coming from two independent trees of length t and V is the energy associated to the addition of a new site. For the partition function one can find a similar recurrence:

$$Z_{t+1} = e^{-\beta V} (Z_t^{(1)} + Z_t^{(1)}) \quad (54)$$

where V is as above the energy due to addition of the new site and $Z_t^{(1)}$ and $Z_t^{(1)}$ are two independent partitions function associated to the two smaller trees.

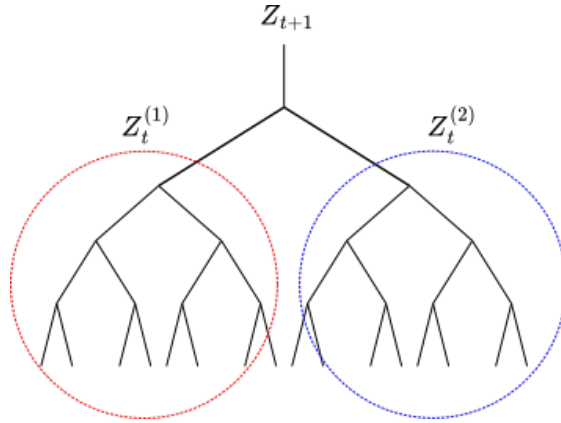


Figure 17: Visual depiction of the recurrence for the partition function.

As done in [7], we can introduce a generating function for Z_t , $G_t(x) = \langle e^{-e^{\beta x} Z_t} \rangle$, which is parametrized by β - the inverse temperature. By taking derivatives w.r.t. x one can obtain the statistics for Z_n . Exploiting the recurrence structure of the partition function one can write:

$$G_{n+1}(x) = \int dV \rho(V) G_n^2(x - V) \quad (55)$$

with $\rho(V)$ the distribution of the V . Conditions for $G_n(x)$ are that $x \rightarrow -\infty G_n(x) \rightarrow 1$ and $x \rightarrow \infty G_n(x) \rightarrow 0$. Hence, it is sufficient to study $G_t(x)$ to gain insights on Z_t . Below we report some of the results.

It was shown in [8, 9, 10] that $G_n(x)$ acquires a travelling wave form linked to the Kolmogorov-Petrovsky-Piskunov (KPP) equation:

$$G_n(x) = w(x + c(\beta)n + r_n) \quad (56)$$

with a velocity $c(\beta)$ depending on the temperature and r_n is a sublinear correction. We report here the main ideas about the derivation of $c(\beta)$. We linearize $G_n(x)$ for $x \rightarrow \pm\infty$ as $G_n(x) = 1 - e^{\beta(x+cn)}$ for $x \rightarrow -\infty$ and by discarding terms of order $e^{2\beta x}$ one can prove that the velocity $c(\beta)$ satisfies:

$$c(\beta) = \begin{cases} v(\beta) & \beta \leq \beta_c \\ v(\beta_c) & \beta \geq \beta_c \end{cases}$$

with:

$$v(\beta) = \frac{1}{\beta} \log \left(2 \int d\tau \rho(\tau) e^{-\beta\tau} \right) \quad (57)$$

and $\beta_c = \arg \min_{\beta} v(\beta)$. This change in the velocity is a type of freezing transition (associated to a one-step replica symmetry breaking) and is of extreme importance in the study of glassy systems. For more details we remind to the original literature [7].

Our interest here is to understand to which extent the DP relations are similar to one examined in this manuscript. For simplicity, one replaces the two variables $s_n^{(1)}$ and $s_n^{(2)}$ by a single one as:

$$x_{n+1} = 1 + s_n(x_n^{(1)} + x_n^{(2)}) \quad (58)$$

Moreover, s_n is promoted to a generic positive random variable. Relabeling $n \rightarrow t$ and mapping $x_n \rightarrow Z_t$ and $s_n \rightarrow e^{-\beta V_t}$ (which is always possible, as $s_n \geq 0$) one recovers a similar recurrence for an "equivalent" partition function

$$Z_{t+1} = 1 + e^{-\beta V_t}(Z_t^{(1)} + Z_t^{(2)}) \quad (59)$$

which one can study with the same techniques as for the DP. Indeed, repeating similar arguments, one finds:

$$G_{n+1}(x) = e^{-e^{\beta x}} \left[\int dV \rho(V) G_n(x - V) \right]^2 \quad (60)$$

The effect of the term $+1$ in the original recurrence is to maintain the value of x_n always above 1. Moreover, it introduces a competition in the growth with respect to disorder. When looking at $G_t(x)$, the $+1$ term, at variance with the DP case, modifies with a β -dependent prefactor the recurrence relation. By looking at $G_t(x)$ again as a travelling wave, the effect of the prefactor is to suppress the right tail of the wave i.e. in the region $x \rightarrow \infty$.

However, as the prefactor depends on β and x explicitly, one can not use the same tools as in the DP case. The study of this modified equation is left for future development, as well as a construction of a continuum (in t) version of the recurrence relation, as already was done previously for the DP [7].

B Importance sampling

As shown in the numerical study of the model, for bigger values of θ ($\theta = 1.50$ and $\theta = 2.00$), corresponding to localized states, the population dynamic approach isn't precise enough to get back the theoretical values of the first two moments of the distribution of x 1314.

To improve the numerical analysis of the pool of x_n , it is used a Monte Carlo method based on importance sampling. The pool at level n is distributed according to:

$$g_n(x) = \frac{\rho_n(x)}{\mu_n(x)} \quad (61)$$

where $\rho_n(x)$ is the real *p.d.f.* of x_n to be determined numerically and $\mu_n(x)$ is a guess for such distribution. From the population dynamics simulations, a power law behavior is expected to occur, which can help set the guess shape for $g_n(x)$.

The procedure that assures that x_n is distributed according to (61) is the following Monte Carlo method:

1. two elements are taken from the pool x_{n-1} and two $s^{(1)}$ and $s^{(2)}$ are generated according to (39) defining a configuration:

$$\mathcal{D} = \{x^{(1)}, x^{(2)}, s^{(1)}, s^{(2)}\} \quad (62)$$

2. $x_n = x[\mathcal{D}]$ is computed using the recursion (33):

$$x[\mathcal{D}] = 1 + s^{(1)}x^{(1)} + s^{(2)}x^{(2)} \quad (63)$$

3. a new configuration is proposed:

$$\tilde{\mathcal{D}} = \{\tilde{x}^{(1)}, \tilde{x}^{(2)}, \tilde{s}^{(1)}, \tilde{s}^{(2)}\} \quad (64)$$

4. the new configuration is accepted with probability:

$$p_{accept}(\mathcal{D} \rightarrow \tilde{\mathcal{D}}) = \min \left[\frac{\mu_{n-1}(\tilde{x}^{(1)})\mu_{n-1}(\tilde{x}^{(2)})}{\mu_{n-1}(x^{(1)})\mu_{n-1}(x^{(2)})} \times \frac{\mu_n[\mathcal{D}]}{\mu_n[\tilde{\mathcal{D}}]}, 1 \right]. \quad (65)$$

$\mu_n(x)$ is taken constant at the first step ($\mu_1(x)$).